Damascus University Journal for engineering sciences
208-195 number (1) -2025: 1 Vo 4

مجلة جامعة دمشق للعلوم الهندسية
المجلد41 العدد(1) – 2025: 208-195

The Punching Shear Strength of Reinforced Concrete Flat Slab under Moments and Shear

Mariam George Abou kassm[*1] **Abd Al Hamed Kikhea**[2]

*[1]. Master student, Department of structural Engineering, Faculty of Civil Engineering- Damascus University. gmail.com@mariamdeeb.kassm

[2]. Professor in the Department of structural Engineering, Faculty of Civil Engineering- Damascus University.

AbdAlHamedKikhea@Damascusuniversity.edu.sy

Received:17 /11/2022
Accepted:23/3/2023

Abstract:

Eccentric vertical load on a flat slab causes an unbalanced moment called the transferred moment. During the transition, a partial rotation of the slab occurs around the column, an indirect shear is formed in addition to the direct shear, and the punching shear becomes more dangerous.

An analytical study was carried out to investigate the effect of the transferred moment caused by eccentric vertical loads on the punching shear strength of a flat slab without drop supported on a non-continuous middle column, as well as the presence of different levels of column load and the role of longitudinal reinforcement. The study was carried out with the Abaqus software version 6.14 and a nonlinear static analysis.

The study showed that increasing the percentage of longitudinal reinforcement up to 1% leads to a significant increase in the shear strength of the flat slab, especially when the reinforcement bars are concentrated in the critical shear region around the column. According to this paper, the maximum effective width of the critical shear region was determined by a distance equal to 2d + c + 2d. It was found that the load of the column could reduce the indirect shear in cases of high longitudinal reinforcement ratios (up to 1%) and concentrated bars. The study also showed that replacing the concentrated longitudinal reinforcement bars with a steel section embedded in the slab at the column gives similar results in terms of increasing the shear strength, while the results were better when internal steel sheets were used at the end of the distance 2d+c+2d.

Key words: Flat slab, Punching shear strength, Eccentric loading, indirect shear, Transferred moment, critical shear region.

مقاومة بلاطة مسطحة من البيتون المسلح على الثقب تحت تأثير العزوم وقوى القص

مريم جورج أبوكسم*[1] عبد الحميد كيخيا[2]

*[1]. طالبة ماجستير – قسم الهندسة الإنشائية– كلية الهندسة المدنية– جامعة دمشق.

gmail.com@mariamdeeb.kassm

[2]. أستاذ – قسم الهندسة الإنشائية– كلية الهندسة المدنية– جامعة دمشق.

AbdAlHamedKikhea@Damascusuniversity.edu.sy

تاريخ الايداع: 2022/11/17
تاريخ القبول: 2023/3/23

الملخص:

تسبب لامركزية الأحمال الشاقولية على البلاطة المسطحة فرق عزم ينتقل إلى العمود يسمى بالعزم المنتقل او غير المتوازن Transferred Moment أو Unbalanced Moment. أثناء انتقال هذا العزم يحدث دوران جزئي للبلاطة بالمنطقة المحيطة بالعمود ويتشكل قص غير مباشر إضافة للقص المباشر ويصبح الثقب أكثر خطورة.

هذا البحث عبارة عن دراسة تحليلية تتناول تأثير العزم الناتج عن لامركزية حمل شاقولي على مقاومة الثقب لبلاطة مسطحة بدون سقوط، تستند على عمود وسطي غير مستمر، وتأثير هذه اللامركزية في وجود عدة مستويات تحميل للعمود، كما وتظهر دور التسليح الطولي في رفع مقاومة الثقب. تمت هذه الدراسة بإجراء تحليل ستاتيكي لاخطي مستخدمين طريقة العناصر المحدودة بواسطة برنامج الأباكوس نسخة 6.14.

أظهرت الدراسة أن زيادة نسبة التسليح الطولي إلى 1% تؤدي إلى زيادة ملحوظة في مقاومة البلاطة للثقب وخاصة عند تركز قضبان التسليح في منطقة القص الحرجة حول العمود، ووفقاً لهذه الورقة تم تحديد العرض الأعظمي الفعال لمنطقة القص الحرجة بمسافة تساوي 2d+c+2d. بينت الدراسة أن حمولة العمود يمكن أن تخفض القص غير المباشر في حالة نسبة تسليح طولي جيدة (1%) مع التكثيف. أظهرت أن استبدال التسليح الطولي المكثف بمقطع معدني داخل البلاطة عند الاستناد يعطي نتائج مماثلة من حيث زيادة مقاومة القص، كانت النتائج أفضل في حال استخدام صفائح معدنية داخلية في نهاية المسافة 2d+c+2d.

الكلمات مفتاحية: بلاطة مسطحة، مقاومة الثقب، حمل لامركزي، قص غير مباشر، عزم منقول، منطقة القص الحرجة.

Introduction:

A flat slab is supported directly on the columns without bearing beams. The area around the column transfers shear and moment loads to the column; therefore, it is subjected to high stresses and must be designed so that no local collapse occurs.

Punching shear is a brittle and sudden collapse that occurs at the critical section near the column due to direct shear caused by vertical load. When the spans around the column are not equal or the distribution of vertical loads is not symmetrical, as in most buildings, this leads to an unbalanced moment that is transmitted to the column to complete the balance, called the transferred moment. During the transition, a partial rotation of the slab occurs in the area around the column, and an indirect shear is formed as shown in Fig. 1. As a result, the punching shear becomes more dangerous.

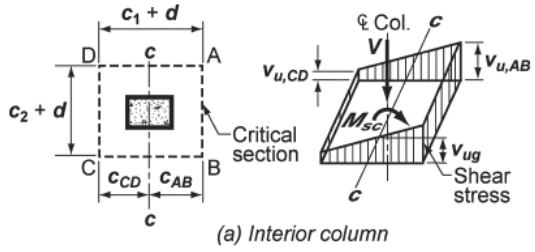

Fig(1) The result of the direct and indirect shear at the critical section[3]

If the slab around the column is rigid, it will resist rotation; in addition, the unbalanced moment will be completely transmitted to the column without forming indirect shear.

The Syrian Arab Code for the Design and Implementation of Reinforced Concrete Structures, Fourth Edition [(1)], determines the part of the unbalanced moment transmitted to the interior and the edge columns of the flat slab in Chapter Eight Clause (4-6-2-f), without addressing the value of the indirect shear in the shear stress formula at the critical section, by the relation:

$$\frac{Vu}{\Omega . b_o . d} < \tau cu \quad ;\Omega=0.85 \qquad \textbf{Eq. (1)}$$

d: the effective depth of the slab at the critical section.

bo: the perimeter of the critical section.

Vu: the ultimate shear force at the critical section.

$\tau cu=0.31\sqrt{fc}$: The allowable shear stress.

However, the European Code EC2 [(2)] takes into account the asymmetrical distribution of shear force by increasing the direct shear by a factor (or by decreasing the shear perimeter) by the given formula:

$$\beta \frac{Vu}{b_o . d} < \tau cu \qquad \textbf{Eq. (2)}$$

β: load increment factor for considering the asymmetrical distribution of shear force in the control perimeter; A general method for determining β is described in EC2 [(2)], Chap. 6.4.3.

Further, the American code ACI 318-14 [(3)] gives separately the value of indirect shear and added to the direct shear value when calculating the shear stresses at the critical section by the given formula:

$$\frac{1}{\Omega .}\left(\frac{Vu}{b_o . d}+\frac{\gamma Mu}{J}\right) < \tau cu \quad ;\Omega=0.75 \qquad \textbf{Eq. (3)}$$

γ: factor less than one.

Codes also differ in defining the location of the critical shear section from the column face. ACI 318-14 [(3)] defines several sections for calculating the two-way shear in flat slabs: in reinforced concrete flat slabs without shear reinforcement, the control perimeter is at d/2 from the column face, and if shear reinforcement is used, the critical section of the shear is located at d/2 away from the last row of the ties or studs, as shown in Fig. 2.

While the European code EC2 [(2)], as shown in Fig. 3, defines the location of the critical section at 2.d away from the column face in the first case and at 2.d away from the last row of ties in the second case. As for the Syrian code [(1)], the critical section is located at d/2 from the face of the column. The code allowed the use of shear reinforcement (ties) in flat slabs but did not address the possibility of shear collapsing outside these ties.

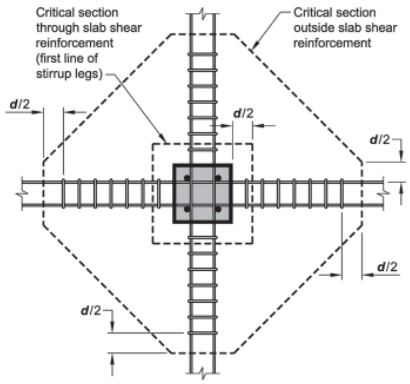

Fig (2).The critical perimeter according to ACI 318-14 [3]

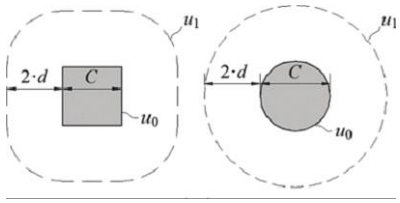

Fig (3) The critical perimeter according to EC2 [2] Case without shear reinforcement

1- Preview studies

The critical shear crack theory, which was proposed by Kinnunen, S., and Nylander, H. (1960) [4] is about the relationship between the punching shear of the flat slab with its deformation due to bending and the amount of the longitudinal reinforcement; therefore, the angle of rotation of the slab.

Muttoni, A., and Schwartz (1991) [5] have been working on this theory and have investigated the influence of slab thickness d on the rotation angle ψ and the influence of the development of flexural cracks near the column, especially in cases of thin slabs and low reinforcement ratio. After that, Muttoni A. (2008) [6] introduced the size effect of the slab by multiplying the slab rotation ψ by its thickness d. "Muttoni proposed that the failure is governed by a parameter ψ. d; this parameter is related to the opening width of flexural cracks due to flexural deformations in the shear-critical region." Fig. 4.

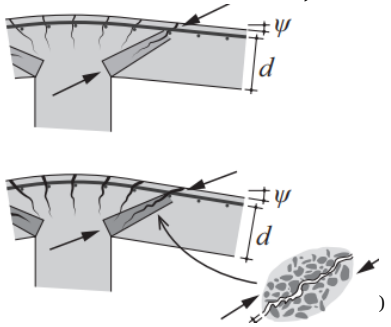

Fig (4) Flexural deformations and cracking close to the column [6]

Einpaul, Ruis, and Muttoni (2015) [7] explained that the samples that have been used in the punching experiments are square and circular with a length of 0.44 L, which represents the hogging moment area around the column between points of contra-flexure, as shown in Fig. 5, where L is the distance between column axes and 0.22 L is the distance between the point of contra-flexure and the column axis. The isolated specimens' boundary condition is to restrict the vertical movement of the ends.

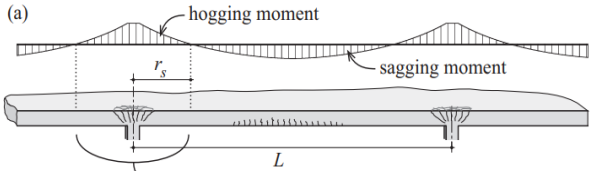

Fig(5) Continuous slab and a corresponding isolated test specimen [7]

Zoran Brujić et al. (2018) [8] conducted an experimental and numerical study to investigate the effects of moment transfer at the flat-slab-inner-column connection for seven specimens without shear reinforcement; the concrete classes of the specimens differed from C30/37, C60/75, and C80/95.

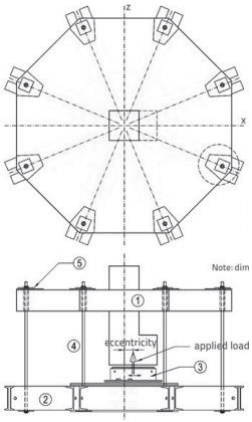

Fig (6) Experiment setup in Zoran Brujić et al [8]

The load was gradually increased as the eccentricity of the load decreased, so that the moment remained constant during the experiment. Fig. 6 shows the experiment setup.

With the aim of developing the shear stress theoretical formula in the presence of the eccentricity, the researchers investigated the effect of the parameter e/b, where e is the eccentricity and b is the diameter of a circle passing through the punching perimeter. The experimental research has shown that increasing the eccentricity reduces the shear resistance of the flat slab and also reduces the control perimeter. An experimental coefficient $k_e = \frac{1}{1+e/b}$ was proposed to reduce the control perimeter. The experimental and numerical results were compared, and the results were acceptable with a difference of 10% except for specimens with large loading eccentricity and low fc. The researchers revealed that the proposal of K_e requires additional experiments.

Al-Katib et al. (2019) [9] conducted an analytical study to model experiments carried out by Kruger et al. (2000) [10] using the 3DNFEA program. The study analyzes the effect of eccentric loading on the punching shear strength of a flat slab in two cases: with U-shaped shear reinforcement and a longitudinal reinforcement ratio of 1.3% compared to a flat slab without shear reinforcement and a longitudinal reinforcement ratio of 1.0%, as shown in Fig. 7.

An eccentric load was increased, the eccentricity remained constant, three different eccentricities were experimented with (0, 150, and 300) mm, and the compression concrete strength was 35 MPa for all specimens. Four different measures of eccentricity were modeled by Al-Katib et al.

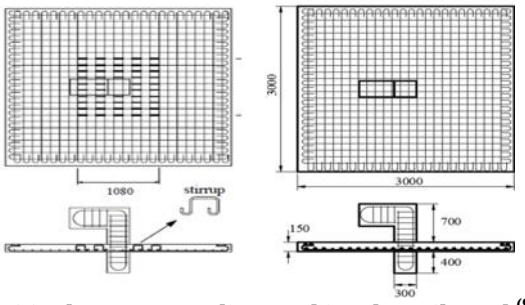

Fig(7) The two cases discussed in Al-Katib et al [9]

This analytical study indicated the possibility of using three-dimensional programs that adopt the method of finite elements to simulate the experience within acceptable accuracy. The results showed that the moment did not affect the elastic stage; the capacity of the slab began to decrease after the first crack using shear reinforcement increased the shear capacity by about 30-35%; however, applying the eccentricity of 160 decreased the shear capacity of the slab by 22% in all specimens, with or without using ties.

Neamah et al., (2021) [11] conducted an experimental study with the aim of studying the behavior of a flat slab with a column capital under bi-axial loading for six specimens, four of them are with a column capital as shown in Fig. 8.

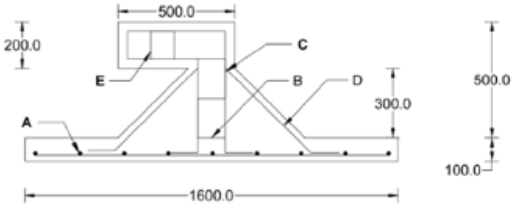

Fig(8) Specimen with column capital (Neamah et al., 2021) [11]

The reference specimen SE0C0 (without column capital) was tested under concentric loading, and SE1C0, similar to the previous specimen, was tested under biaxial loading. Results showed a reduction in shear capacity of 16%. It was observed that the behavior of the specimen was affected by biaxial loading at all stages, including the elastic stage. The remaining specimens with column caps were tested under concentric and biaxial loading. It was found that the presence of column capital significantly increased the shear capacity of the slab by 2.11% and 1.88%, respectively, and that biaxial loading reduced the shear capacity of the slab in all specimens, with or without column capital.

We find from above that the punching shear in flat slabs under eccentric loading is still under development, and the location of the critical shear section is not the same in different international codes, so more research needs to be done.

3-the aim of this paper:

This paper is an analytical study that investigates the effect of the transferred moment resulting from eccentric vertical load on a flat slab without drop supported on a non-continuous middle column, the effect of the moment in the presence of different levels of column load, the role of the ratio, and the arrangement of longitudinal reinforcement. Finally proposing alternatives such as the use of a steel section or steel plates embedded in the flat slab.

4- Structural analysis of a flat slab under increased concentric load

An analytical model was built using Abaqus version 6.14 [12] to simulate the experiment on the reference specimen SE0C0 by Neamah et al. (2021) [11], which was tested under concentric loading. In order to correspond the real behavior of the experiment, the parameters of the Abaqus program were defined by matching the analytical results with the experimental results; these parameters are then adopted in other analytical models when applying the eccentric loading.

Figure 9 shows the dimensions of the experimental specimen SE0C0, which are 1600 x 1600 mm. square slab with a thickness of 100 mm, dimensions of the central column 200x200 mm, and the flexural reinforcement is bottom mesh ratio 0.55% (9 Ø10 mm rebar in each direction). Table 1 shows the reinforcement of the experimental specimen SE0C0.

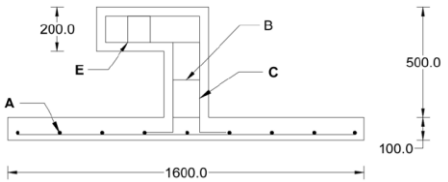

Fig(8) Dimensions of the Experimental Specimen SE0C0 (Neamah et al., 2021) [11]

Table (1) The reinforcement of the experimental specimen SE0C0 (Neamah et al., 2021) [11]

Reinforcement	Details
A	9ø10mm @ 190mm c/c
B	closed stirrups 3ø12mm @ 110mm c/c
C	4ø12mm
E	closed stirrups 2ø12mm @ 100mm

Figures (11) and 12 show the analytical model and the reinforcement in Abaqus.

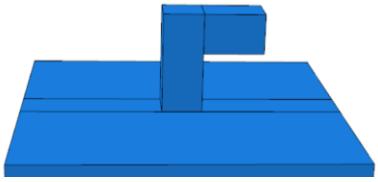

FIG (11) The analytical model in Abaqus

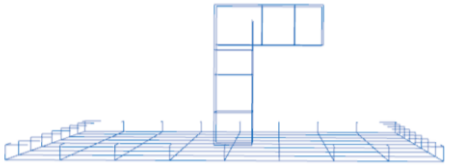

FIG (12) The reinforcement in Abaqus

To model the slab, a three-dimensional element of eight nodes was used; each node had six degrees of freedom (three transitions and three rotations) (C3D8R, an 8-node linear brick, reduced integration), and the linear element (T3D2, a two-node linear displacement, truss elements) was used to model the reinforcing bars. The rebar was considered embedded in the concrete with the assumption of complete coherence. The concrete material was characterized in Abaqus by the CDP as shown in Figure 13, which is a general method of modeling the inelastic behavior of concrete that can be used in monotonic loading.

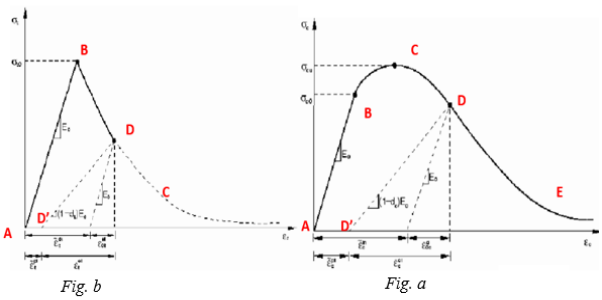

[ABAQUS V6.14 Documentation]

FIG (13) Concrete Damage Plasticity Model [12]

a. Compression behavior associated with compression hardening;

b. tension behavior associated with tension stiffening

The same properties were used as those used in the reference experimental study for concrete and steel materials. The cubic compressive strength of concrete is 33 MPa for 150x150x150 cubes; by taking a correction factor of 0.80, the corresponding cylindrical compressive strength is 26.5 MPa, the modulus of elasticity is 28 GPA, and the Poisson's ratio is 0.2. Figure 14 shows the concrete stresses and plastic strains corresponding to the experiment.

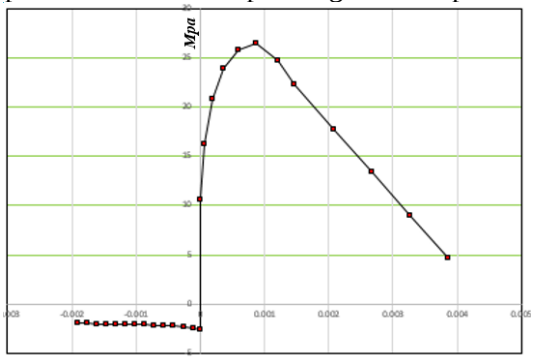

Fig (14) Stress-plastic strain used to define the concrete material

The steel's yield strength is Fe500, its modulus of elasticity is 210 GPA, and its Poisson's ratio is 0.3. Figure (15) shows the behavior of steel material: elastic-perfectly Plastic.

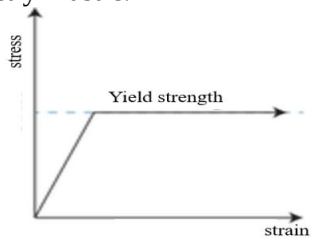

Fig(15) Stress-strain for steel material

Also, the same boundary condition that was used in the experiment was adopted in the numerical model, where the vertical movement at the ends of the slab was inhibited by $U_y = 0$, as shown in Figure (16).

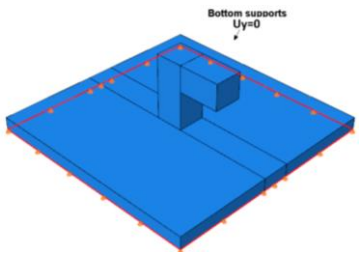

FIG (16) The boundary conditions

In the model, the weight was applied at step 1, then at step 2, the concentrated vertical load was increased gradually over time. Nonlinear static analysis was performed using the finite element method. The mesh of elements has been studied with the aim of reaching a good division that achieves accuracy in results and is economical in time; the 50x50 division was adopted, which gives converging results.

5-Comparison of analytical and experimental results in the case of increased central load:

Table (2) shows the results of the SEOCO reference experiment. [10]

Slab	Ultimate load (P_u) kN	Deflection mm
SE0C0	122	18.31

Table (3) shows the analytical result from Abaqus.

	maximun load KN	displacement mm
Abaqus	121.59	17.7

Figure (17) shows a comparison between the analytical shear force from Abaqus and the experimental result; the horizontal axis represents the vertical displacement of the slab in mm, and the vertical axis represents the shear in KN.

From the figure, we can see the similarity of the values in the two curves; this indicates the reinforced concrete material was modeled in a way that approximates the real behavior of the experimental concrete. The slight difference is due to shrinkage cracks that formed when pouring the specimen, which were not taken into account in the analytical study.

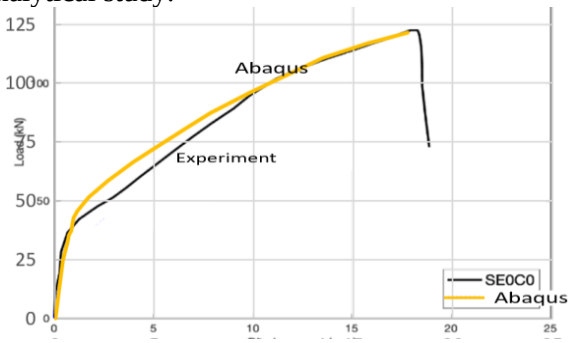

FIG(17) Comparison of the analytical result with the experimental result

Figure 18 shows the PE (principal maximum) maximum plastic deformation resulting from the analytical study on the tensile surface compared to the crack pattern in the specimen SE0C0. The density of cracks around the column forming the punching shear can be seen.

FIG(18)

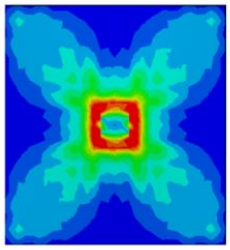

PE (principal maximum) from this analytical study

SE0C0 Neamah et al., (2021) [11]

The shifting of the maximum plastic deformation toward the applied load was observed with the change in the shape of the punching shear. (figure20)

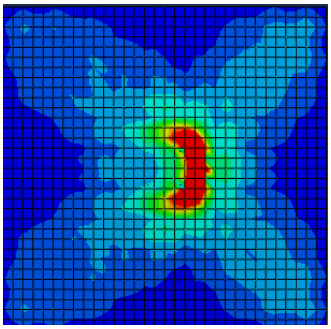

FIG (20) PE (principal maximum) on the tensile surface

6-Structural Analysis of a Flat Slab under Increased Eccentric Load

In this analysis, the same definitions of previously used elements, materials, and boundary conditions were preserved, except the loading is eccentric. The load has gradually increased over time, while the eccentricity remains constant. Two cases were studied: e_1 = 150mm, e_2 = 250mm. Figure (19) shows the relationship between shear force and displacement in the e_1 and e_2 cases and their comparison with the case e_0. We notice the eccentricity causes an indirect shear, which is the distance between the curve e_0 and the curves e_1, e_2, according to the studied case. The shear capacity decreased by 12.6% at e_1= 150mm, and by 23.2% at e_2 = 250mm.This decrease is not linear, and that indirect shear has been limited to the inelastic stage.

FIG(19)

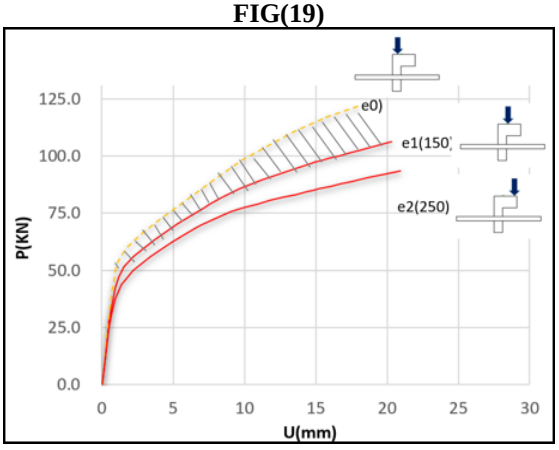

7-Structural Analysis of a Flat Slab under Eccentric Load at Different Column Load Levels:

In this analysis, the same definitions of previously used elements, materials, and boundary conditions were preserved except the loading was applied as following:

1- Self-weights was applied as step1.

2- In step2, the part (0.25) of the total force P, was applied at the column and was gradually increased.

3- In step3 after the application of the column load was completed, the rest of the total load (0.75) of the total force P was applied at a specified distance so that the total loads p had an eccentricity of e=250mm, the load was gradually increased over time.

In order to study several column load levels, the previous analysis was repeated several times with the use of (0.4) of the total force P in step 2, (0.6) of the total force P in step 3, and the maintenance of total eccentricity e = 250mm. Finally, the analysis was repeated again with (0.5) of the total force P in step 2, (0.5) of the total force P in step 3, and the total eccentricity e = 250mm. Figure (21) shows the load protocol at each level.

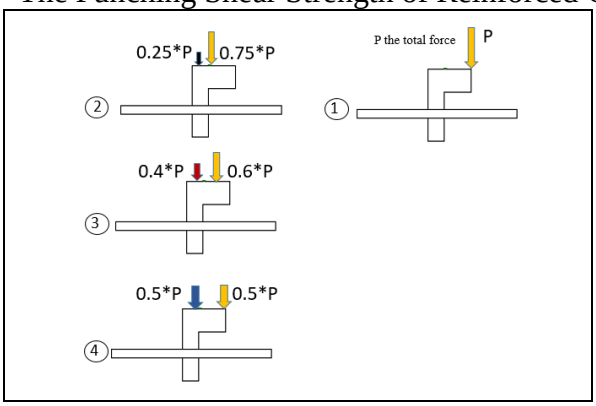

Fig(21) The load protocol at each level (P: the total force in kN)

Table(4)shows different load levels.

Level	Column Load	Eccentric Load	The Distance	The Eccentricity
1	0	P	250	250
2	0.25*P	0.75*P	333	250
3	0.4*P	0.6*P	417	250
4	0.5*P	0.5*P	500	250
unit	KN	KN	mm	mm

The results are presented in Figure 22 and compared with the result of a central load at e = 0. We find from the figure that the moment due to eccentricity causes in all cases an indirect shear and that increasing the column load level of a flat slab with a reinforcement ratio of 0.55% had a slight effect in reducing indirect shear (7% within a load up to half of the total load).

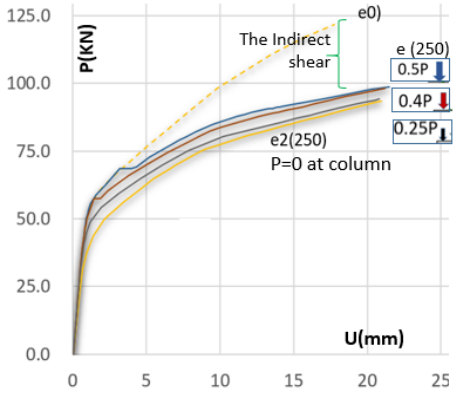

Fig (22) Effect of e = 250mm under several column load levels and a 0.55% reinforcement ratio

8- Effect of Flexural Reinforcement

The effect of flexural reinforcement was investigated through conducting several structural analyses using the finite element method on a flat slab under eccentric load according to the following cases:

8-1-the increasing of the flexural reinforcement ratio:

In the previous structural analysis, the flexural reinforcement ratio was 0.55% (9T10 within the length of 1600 mm); in this analysis, several slabs under the constant eccentricity e=250 mm will be used using different reinforcement ratios up to 1% by increasing the number of reinforcing bars. Table 5 shows the number of bars corresponding to the reinforcement ratios used.

Table (5)

ratio	0.55%	9T10	
ratio	0.70%	12T10	increasing the number of bars.
ratio	0.90%	15T10	increasing the number of bars.
ratio	1.00%	17T10	increasing the number of bars.
ratio	1.00%	9T14	increasing the diameter

We can see from the previous table that the ratio of 1% was used in two ways: the first by increasing the number of bars and the second by increasing the diameter. Figure (23), which shows the results of the maximum shear force of the slabs, indicates that increasing the reinforcement ratio by increasing the number of bars increases the shear capacity of the slabs, while increasing the reinforcement ratio by increasing the diameter does not give the same value. For example, the ratio of 1% indicates the importance of the bars distributed in a certain area of the slab.

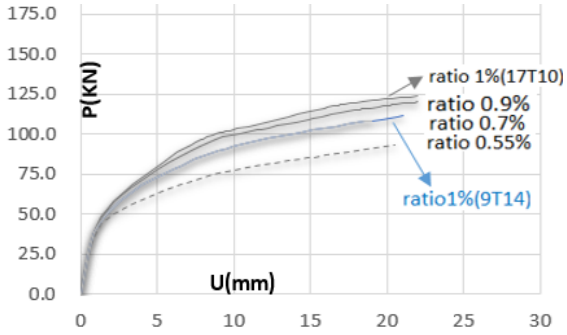

Fig (23) Effect of the Reinforcement Ratio

8-2.: The Concentrating of the Flexural Reinforcement under Eccentric Load

In order to find the optimal distribution of longitudinal reinforcement and determine the effective width of the slab to resist the punching shear under eccentric load at different column load levels, bars above the ratio of 0.55% were concentrated at several distances near the column. A

comparison was made between the 15T10 uniformly distributed over the entire width and the 9T10 uniformly distributed plus the 6T10 concentrated within a distance of (3.5d, 2d, d) from each face of the column, as shown in Figure (24), where d is the effective slab height and c is the width of the column.

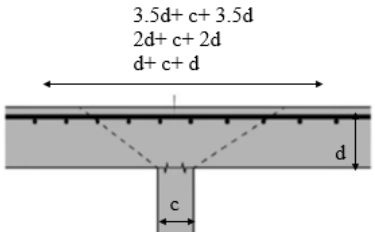

Fig (24) The concentrated distances

Figures 25–27 illustrate the distribution of bars in the studied cases.

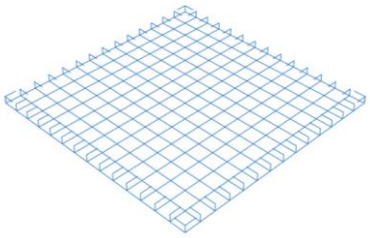

Fig(25) uniformly distributed

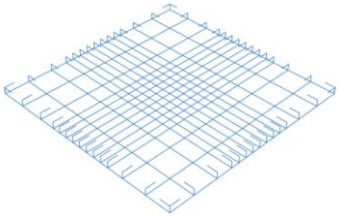

Fig(26) Concentrated within (2d+c+2d)

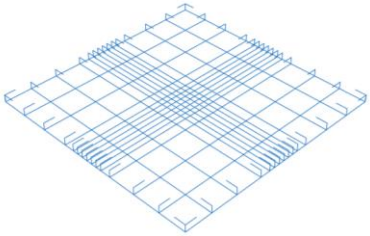

Fig(27) concentrated within (2d+c+2d)

Figure (28) shows the results of the maximum shear force of the slabs; We found that the smaller the concentrated width, the higher the shear capacity of slabs, the values converge at concentrated equal to or smaller than (2d+c+2d), therefore the maximum effective width of condensation can be considered equivalent to (2d+c+2d).

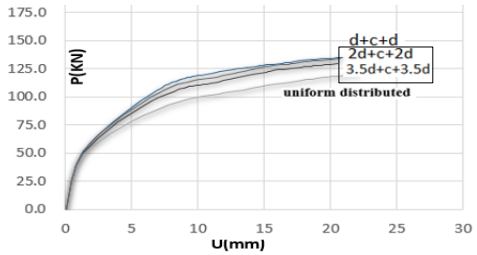

Fig (28) Effect of the Concentrated Bars

We note from figure (29) that for a slab with a reinforcement ratio of 0.9% with condensation within (2d + c+ 2d), the shear resistance was increased by more than (1.7) times in the case of e = 0 and by (1.45) in the case of e = 250 mm compared to a reinforcement ratio of 0.55%. So we do not recommend using a low reinforcement ratio. However, the eccentricity reduced the shear capacity of the slab in all cases.

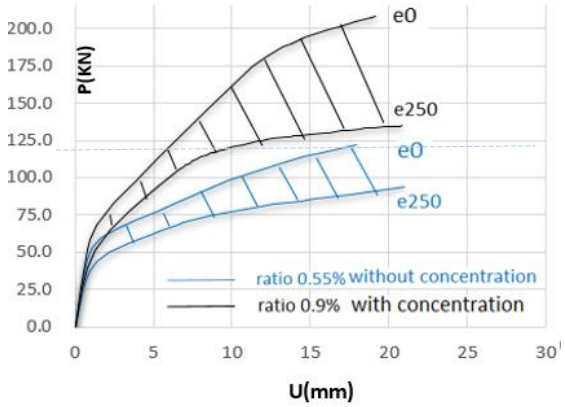

Fig (29) Comparison between a reinforced slab of ratio 0.55% without concentration and another of ratio 0.9% with concentration

8-3.: The Concentrating of the Flexural Reinforcement under Eccentric Load at Different Column Load Levels:

A flat slab with a reinforcement ratio of 0.9% and concentrated bars at a distance of (2d + c + 2d) was analyzed under the loading protocol mentioned in paragraph 7. We can see from Figure 30 that increasing the column load decreases the indirect shear and improves the shear capacity.

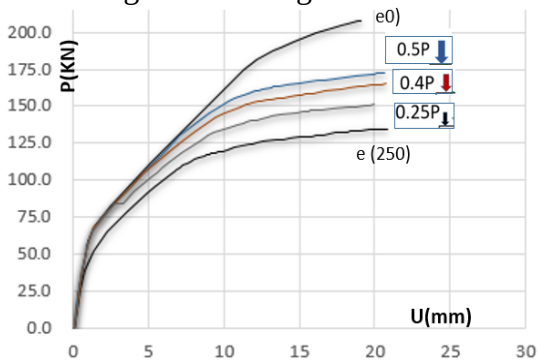

Fig (30) The impact of column load levels

We concluded from the above that increasing the reinforcement ratio up to 0.9-1% activated the column load to reduce the indirect shear. This is good in practice since the eccentricity load is actually associated with a central load of the column.
9: The Proposal of Replacing the Concentrated Reinforcement with a Steel Section embedded at the support:
In this analysis, the same definitions of elements, materials, and boundary conditions used previously were used with the addition of an element that is a steel section. The steel section RHS 50X30X3.2 is equivalent to the area of the concentrated bars (6T10). Figure 31 shows the RHS section, and Table 6 shows the specifications of this section according to BS EN 10210-2 (2006) [13].

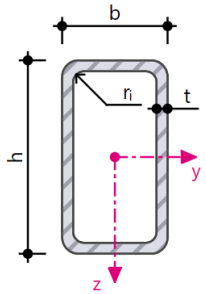

FIG (31) RHS 50X30X32mm [13]

Table (6) according to BS EN 10210-2 (2006) [13]

RHS 50x30x3.2 ▪ BS EN 10210-2:2006			
Depth	h	50.0	mm
Width	b	30.0	mm
Thickness	t	3.2	mm
Outer corner radius	r_o	4.8	mm
Inner corner radius	r_i	3.2	mm
Sectional area	A	4.60	cm^2
Weight	G	3.6	kg/m
Plastic section modulus about y-axis	$W_{pl,y}$	7.24	cm^3
Plastic section modulus about z-axis	$W_{pl,z}$	5.00	cm^3
Area moment of inertia about y-axis	I_y	14.20	cm^4
Area moment of inertia about z-axis	I_z	6.20	cm^4

To model the RHS steel section, a three-dimensional element of eight nodes was used; each node had six degrees of freedom (three transitions and three rotations) (C3D8R, an 8-node linear brick, reduced integration). The RHS was considered embedded in the concrete with the assumption of complete coherence. The steel's yield strength is Fe500, its modulus of elasticity is 210 GPA, and its Poisson's ratio is 0.3. A structural analysis was performed; the load has gradually increased over time while the eccentricity remains constant. Figure 32 shows the shape of the steel section used, Figure 33 shows the reinforcement of the slab in Abaqus, and Figure 34 shows the relationship between the force-displacement of the slab with embedded RHS compared to the result of the concentrated bars within the distance of (2d + c + 2d) shown earlier in Figure 28.

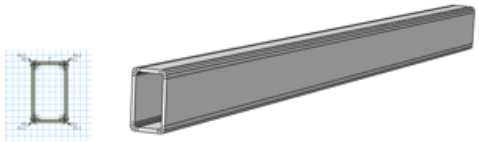

Fig (32) The shape of an RHS steel section in Abaqus

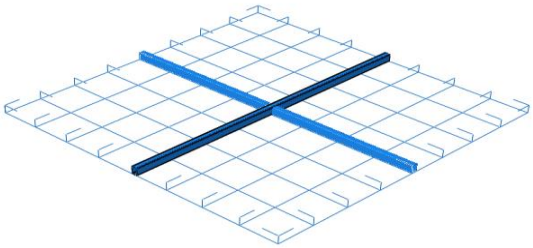

Fig (33) A uniform reinforcement 9T10 (ratio of 0.55%) and the embedded RHS

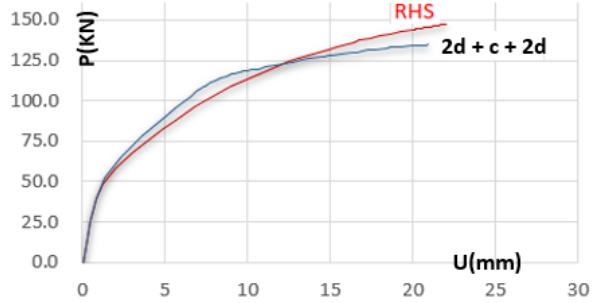

Fig (34) A comparison between the shear capacity of a flat slab with an embedded RHS section and the use of concentrated bars

From the previous figure, we see a convergence in the behavior of the two models where the two curves match in the elastic stage and then, at the beginning of the inelastic stage, the curve corresponding to the use of the RHS steel section decreased slightly and then the two curves converged with the same result, and in the final stage the performance of the RHS model improved slightly. Figure 35 shows the tensile stresses in reinforcing steel, where in both cases, the yielding point was reached in the failure.

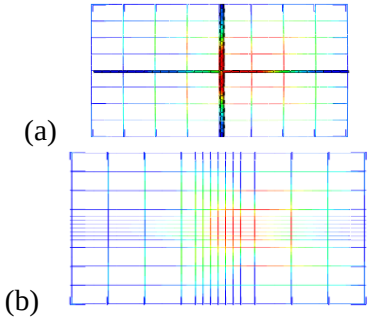

Fig (35) The tensile stress in the reinforcing steel

a- RHS model

b- Concentrated bar model

10. The Proposal of Replacing the Concentrated Reinforcement with Steel Plates Embedded at Each End of (2d + c + 2d):

In this analysis, the same definitions of elements, materials, and boundary conditions used previously were used with the addition of steel plates. Two embedded steel plates of dimensions 2 x 100 x 2.25 mm, which are equivalent to the area of the concentrated bars (6T10), were placed at the end of (2d + c + 2d). Figure 36 shows the location of the plates.

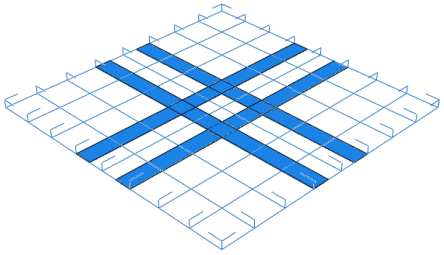

Fig (36) the location of the plates.

The C3D8R element was used to model the plate; the plate was considered embedded in the concrete; the steel's yield strength is Fe240; its modulus of elasticity is 210 GPA; and its Poisson's ratio is 0.3. A structural analysis on a flat slab with a constant eccentricity of 250 mm was performed. Figure 37 shows the relationship between shear force and displacement in the three cases.

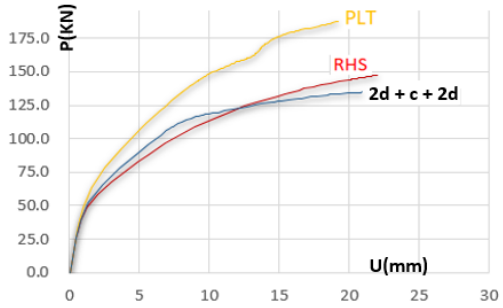

Fig (37) A comparison between the shear capacities in the three cases

We conclude from previous results that the use of plates at a distance (2d+c+2d) gives the best shear capacity.

11: The Results:

This study showed the following results:

1. The punching resistance is increased by the flexural bars, which are concentrated in the shear critical area over and around the column.
2. In this study, the maximum width for the shear critical area was found to be (2d + c + 2d) under the eccentricity of 250mm, where d is the effected slab thickness and c is the width of the column.
3. When eccentric loads are accompanied by column loads, the indirect shear force would be reduced only in cases of high reinforcement ratios (up to 0.9%) and concentrated bars in the distance (2d + C + 2d).

4. Replacing the concentrated reinforcement with a RHS steel section embedded at the support gave the same result in raising the punching resistance.
5. Replacing the concentrated reinforcement with steel plates embedded at each end of the width (2d + c + 2d) gave the best shear capacity in the case of eccentricity e = 250mm.

Recommendations:

According to the Syrian code, when designing a flat slab similar to the one studied in this paper, the allowable shear force, according to Eq. 1 in the introduction, is vu = 121 kN, regardless of the ratio of longitudinal reinforcement of the slab or the moment transferred to the column. In fact, the slab would be punctured at a lower value, at the value of 93 kN, in the case of low reinforcement with eccentricity e = 250 mm, as we have seen in this study (Fig. 29).

We recommend that the effect of the longitudinal reinforcement ratio be entered in the calculation of the punching shear force according to the Syrian code. Also, the design should consider the effects of a transferred moment.

Funding: this research is Funded By Damascus University- Funder No (501100020595).

References:

(1) - Syrian Engineers Union (2012), Syrian Arab Code for the Design and Implementation of Reinforced Concrete Structures, 4th Edition, Engineers Union, Damascus.

(2) - Eurocode 2: Design of Concrete Structures, Part 1-1: General Rules and Rules for Buildings; EN 1992-1-1: 2011-01.

(3) - Building Code Requirements for Structural Concrete (ACI 318-14) and Commentary (ACI 318R-14).

(4) - Kinnunen, S., and Nylander, H., "Punching of Concrete Slabs Without Shear Reinforcement," Transactions of the Royal Institute of Technology, No. 158, Stockholm, Sweden, 1960, 112 pp.

(5) - Muttoni, A., and Schwartz, J., "Behaviour of Beams and Punching in Slabs without Shear Reinforcement," IABSE Colloquium, V. 62, Zurich, Switzerland, 1991, pp. 703-708.

(6) - Muttoni, A.: Punching Shear Strength of Reinforced Concrete Slabs without Transverse Reinforcement, ACI Structural Journal, 105 (2008) 4, pp. 440–450.

(7) - Einpaul, J., Fernández Ruiz, M., & Muttoni, A. (2015). Influence of moment redistribution and compressive membrane action on the punching strength of flat slabs, Engineering Structures, 86, 43–57, doi:10.1016/j.engstruct.2014.12.032
.

(8) - Zoran Brujić et al. (2018). Punching shear strength of eccentrically loaded RC flat slabs without transverse reinforcement. Journal of the Croatian Association of Civil Engineers, 70(09), 757–770, doi:10.14256/jce.2404.2018.

(9) - Al-Katib, H. A. A., Alkhudery, H. H., & Al-Katib, A. A. A. (2019). Flat Slab–Column Modeling Using Finite Element with Eccentric Loading Effects. Iranian Journal of Science and Technology, Transactions of Civil Engineering, doi:10.1007/s40996-019-00249-z.

(10) - Krüger G, Burdet o, and Favre R (2000) Punching strength of R.C fat slabs with moment transfer. In: Int. work. Punching Shear, pp. 1–8.

(11) - Neamah et al. (2021). Punching shear strength of flat slab strengthened with reinforced concrete column capital under bi-axial loading. IOP Conf. Series: Materials Science and Engineering, Sci. 1067-012005.

(12) - ABAQUS, Version 6.14 "ABAQUS/Standard User's Manual," ABAQUS Inc., USA.

(13) - BS EN 10210-2 May 31, 2006 Hot finished structural hollow sections of non-alloy and fine grain steels - Part 2: Tolerances, dimensions and sectional properties.